

## Upstream separation in a rotating channel flow

K. M. Borenäs

Department of Oceanography, Earth Sciences Centre, Göteborg University, Göteborg, Sweden

J. A. Whitehead

Department of Physical Oceanography, Woods Hole Oceanographic Institution, Woods Hole, Massachusetts

**Abstract.** The question of upstream separation of a current of dense rotating fluid, below a stagnant layer of lower density, that is critically controlled by a weir is addressed in laboratory experiments that follow from theoretical calculations. For a constant potential vorticity flow in a gradually varying channel, it is shown that a range of parameters lead to upstream separation. In all cases the flow reattaches before reaching the sill crest, so that a closed gyre is produced. In laboratory experiments separation and reattachment was observed in numerous cases where the theory predicts closed gyres. Although the shape and size of the gyre are in accordance with theory, the circulation within the gyre differs markedly from theoretical predictions. The mechanism that feeds energy into the gyre appears to be an important unsolved problem. The results indicate that upstream separation is a fact and that the dynamics of the gyre is significant, so the gyre dynamics may modify the volume flux of fluid over the weir.

### 1. Introduction

In the ocean a number of flows through deep passages appear to be topographically controlled. The physical situation which may lead to the formation of such currents is accumulation of dense water in a basin either from surface cooling (possibly aided or dominated by salinity increase as well) or from being fed by inflow from an adjacent basin. The dense water so accumulated lies below a depth which is a few tens or hundred meters higher than the depth (actually the saddle point depth) of the deepest exit passage. Such a picture applies to flows found in Denmark Strait, Discovery Gap, Faroe Bank Channel, Ceara Abyssal Plain, Romanche Fracture Zone, Vema Channel, and the Samoan Passage.

For the last 2 decades the theory of rotating hydraulics has been developed for geophysical sill flows, of the type described above, for which the Earth's rotation is not negligible [see, e.g., Gill, 1977; Pratt and Lundberg, 1991; Borenäs and Pratt, 1994]. The results have been used to estimate the maximum transport of dense bottom water through the passages. Whitehead [1980] (also J.A. Whitehead, Topographic control of oceanic flows in deep passages and straits, submitted to *Reviews of Geophysics*, 1996) compared the theoretical predictions for a flow in a slowly varying channel of rectangular cross section with observations from the aforementioned straits. The theory for a channel of parabolic cross section has also been used to estimate the maximum flow rate through the Faroe Bank Channel [Borenäs and Lundberg, 1988].

The hydraulic theory predicts that a controlled flow of constant (but nonzero) potential vorticity may, for certain parameter ranges, separate from the right-hand wall (looking in the downstream direction with the northern hemisphere sense of rotation). For flows that are unidirectional in the upstream basin, only the

presence of a sill can give rise to this separation, which takes place on the upstream side of the control section. The decrease in depth experienced by the fluid as it approaches the saddle point of the sill is accompanied by a change in the relative vorticity. If the cross-channel shear of the along-channel velocity gets large enough, a stagnation point forms at the right-hand wall, and separation occurs. The flow will, however, reattach before reaching the sill crest. This latter redistribution of the velocity (coupled to a redistribution of the fluid depth across the channel) is necessary to get the fluid across the sill at that specific flow rate.

It has usually been assumed that the streamlines in the separated region have the same potential vorticity as the streamlines emanating from the upstream reservoir and that the fluid recirculates in this area [see, e.g., Gill, 1977; Borenäs and Pratt, 1994]. Another alternative is that the potential vorticity in this region differs from the rest of the fluid and that the separating streamline demarcates, for example, a stagnant pool of water [Borenäs, 1983].

So far there is no conclusive support for any of the alternatives. Borenäs [1983] studied a subcritical, one-layer channel flow over a sill in laboratory experiments and could not detect a reversal flow, although the fluid did separate from the right-hand wall (again looking in the downstream direction). There have been some evidence of reversal flows in oceanic sill regimes. Borenäs and Lundberg [1988] found that in the Faroe Bank Channel the along-channel velocity demonstrated a large cross-channel shear and negative velocities on the right-hand side were found at times. In the Faroe-Shetland Channel, negative velocities have been observed in the deep water on the right-hand flank [Saunders, 1990]. Geostrophic calculations based on the hydrography in this area also show negative velocities on this side of the channel [Schlichtholz and Jankowski, 1993]. By using an inverse method, van Aken [1988] determined the transport of water masses through the Faroese Channels and arrived at a flow pattern in the bottom water which demonstrates a large area of recirculating water.

Relatively few laboratory studies have been conducted of controlled rotating flows; the existing ones are reviewed by Pratt

Copyright 1998 by the American Geophysical Union

Paper number 97JC02548.  
0148-0227/98/97JC-02548\$09.00

and Lundberg [1991]. Whitehead et al. [1974] found experimental agreement with predictions for volume flux from zero potential vorticity theory (or the deep reservoir-narrow channel limit [cf. Borenås and Pratt, 1994] to within tens of percent. They also obtained qualitative observations of the interface configuration that appeared to agree with the shape of predicted interfaces. Their apparatus had many limitations, though, and the parameter range was relatively limited. Furthermore, it was not clear that friction was completely negligible. At the time, only predictions from zero potential vorticity theory existed. The apparatus was made with a very deep upstream basin to produce this condition. However, the very deep upstream basin had the second simplifying effect of producing small upstream flow velocities, so that the upstream interface remained relatively undeformed.

Shen [1981] conducted experiments in a considerably improved apparatus and found more precise verification of both volume flux measurements and interface configurations. As in the first experiments, the apparatus was made with a very deep upstream basin, and thus the results could only be compared with the zero potential vorticity theory. More general theories with constant upstream potential vorticity were developed by then [Gill, 1977], but they included upstream localized currents and it may not have been known how to produce those conditions in the laboratory.

Whitehead [1986] studied the effect of the shear that a flow develops as bottom depth decreases at a sill. In the limit when the Rossby radius of deformation of the surface is still much greater than the width of the tank, shear of sufficient strength can alter the control properties of the flow at the crest of the weir; and Whitehead [1986] found and verified a number of controls, including "geostrophic control" [Garrett and Toulany, 1982]. The experiment utilized an upstream source consisting of water pumped through a porous diffusor. It was found that upstream flow with controlled potential vorticity could be generated with the device.

Pratt [1987] studied shock waves in the lee of a smooth weir in a rotating flume. To produce upstream flow with constant potential vorticity, water was introduced from beneath a sluice gate, from where it flowed through a screen and into a deep region upstream of the smooth weir. The objective was to study the effect of wall separation to hydraulic jumps. (This type of separation, in which case the lower layer ceases to wet the wall and bottom on the left-hand side of the channel, should not be confused with the separation discussed in the present paper, which is caused by stagnation on the right-hand wall.

The aim of the present paper is to theoretically investigate upstream separation of a controlled flow of constant (but nonzero) potential vorticity and to experimentally determine whether separation actually takes place and if rotating hydraulic theory is applicable for this part of the flow.

The outline of the paper is as follows. In section 2 the theoretical model is presented, and the question of upstream separation is dealt with in section 3. The experimental setup is described in section 4, and in sections 5 and 6 the theoretical flow field outside and within the separated area is compared with the experimental results. A discussion in section 7 completes the paper.

2. Theoretical Model

The derivation of the flow properties of a hydraulically controlled flow has been presented in several papers [see, e.g., Gill, 1977] and will only be summarized here.

Consider the flow along a gradually varying channel aligned in the y direction (see Figure 1). The system is one of an active lower layer with a passive layer on top. The channel, of width w, has a rectangular cross section and rotates with constant angular speed f/2. The flow is in geostrophic balance, and the potential vorticity is constant (but nonzero). Nonlinear terms are introduced by the Bernoulli equation for energy conservation. Together with the continuity equation the flow is described, for given geometry and upstream conditions, in terms of an average depth  $\bar{D}$  defined by

$$\bar{D} = \frac{1}{2} \left[ D \left( \frac{w}{2} \right) + D \left( \frac{-w}{2} \right) \right].$$

The value of  $\bar{D}$  is obtained by solving the following equation, which is equivalent to equation 5.13 of Gill [1977]:

$$\frac{2f\psi_i}{g' D_\infty^2} + t^2 \left[ \frac{\bar{D}}{D_\infty} - 1 \right]^2 + \left( \frac{fQ}{2g' D_\infty} \right)^2 \frac{1}{t^2 \bar{D}^2} + 2 \left[ \frac{\bar{D}}{D_\infty} - 1 + \frac{\Delta}{D_\infty} \right] = 0 \quad (1)$$

Here  $t = \tanh(w/R)$ , where  $R = 2(g'D_\infty)^{1/2}/f$  is the Rossby radius of deformation. The reduced gravity is  $g' = g \delta\rho/\rho$ , with  $\delta\rho$  representing the density difference between the two layers. The potential depth (i.e., the depth in a hypothetical upstream region at which fluid velocity has zero curl) is denoted  $D_\infty$ . The second upstream parameter,  $\psi_i$ , determines how much fluid is supplied from the right-bank flux compared to the left-bank flux. The

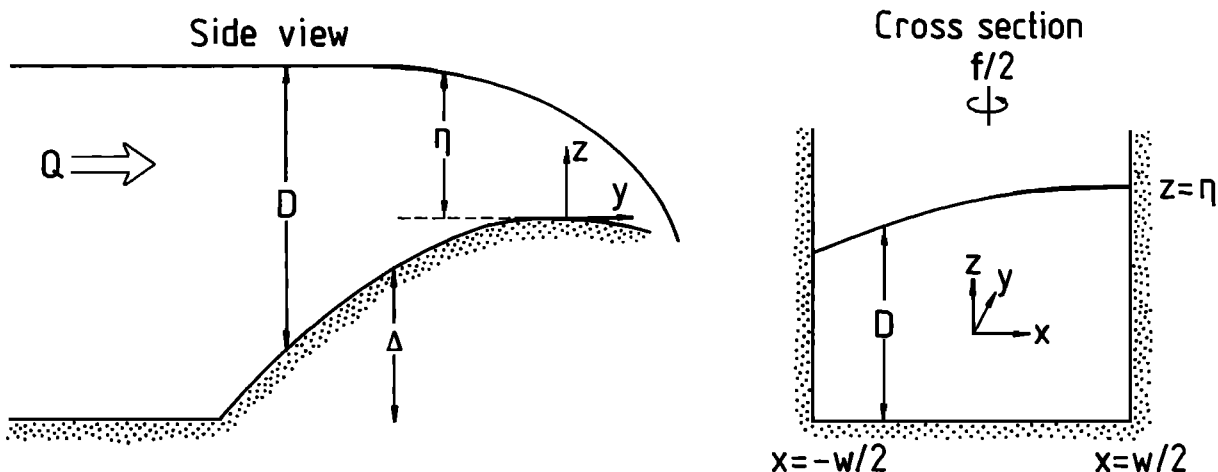


Figure 1. Geometrical notation.

height of the channel floor above the upstream level is  $\Delta$ . The flow rate is  $Q$  and a stream function is defined by

$$Du = -\frac{\partial\psi}{\partial y}, Dv = \frac{\partial\psi}{\partial x}, \psi\left(\frac{-w}{2}\right) = \frac{-Q}{2}, \psi\left(\frac{w}{2}\right) = \frac{Q}{2}.$$

The solution of (1) is multivalued and represents subcritical and supercritical flow, respectively. The two branches coalesce into a branch point at which the solution describes a physical flow only if it is obtained for a sill crest geometry (the control section). For this solution the transport is maximized, which may be expressed by the additional relation

$$D_c = \frac{(fQ/2g')^2 - t_c^4 \bar{D}_c^4}{t_c^2 \bar{D}_c^3 (1 - t_c^2)} \quad (2)$$

where the index "c" stands for control. The velocity along the channel, derived from the geostrophic relation, is

$$v = (g' D_c)^{1/2} \left[ \left( \frac{\bar{D}}{D_c} - 1 \right) \frac{\sinh(2x/R)}{\cosh(w/R)} + \frac{fQ}{2gD_c} \frac{1}{\bar{D}} \frac{\cosh(2x/R)}{\sinh(w/R)} \right] \quad (3)$$

where  $\bar{D}$  is obtained from (1) [cf. Gill, 1977].

On the upstream side of the sill, only the subcritical solution represents a stable flow, and hence this solution is chosen.

### 3. Upstream Separation

A flow which is unidirectional in the far upstream basin can only separate from the right-hand wall. This result is obtained by putting  $v=0$  in the Bernoulli function for the streamlines along the walls and then excluding solutions for which the sill height,  $\Delta$ , becomes negative.

From (3) it follows that when the velocity is zero at the right-hand wall ( $x=w/2$ ), the value of the depth,  $\bar{D}_{v=0}$ , is given by

$$\bar{D}_{v=0} = \frac{D_c}{2} \pm \left( \frac{D_c^2}{4} - \frac{fQ}{2g' t^2} \right)^{1/2}. \quad (4)$$

The corresponding values of the sill height are obtained from (1). The flow separates at the lower sill height and reattaches for the larger value.

In Figure 2, curves dividing the separated from the nonseparated flow have been constructed for different values of the nondimensional flow variable  $\hat{D}_c$  defined as

$$\hat{D}_c = \left( \frac{2g' D_c^2}{fQ} \right)^{1/2}.$$

The diagrams are presented in  $t-\Delta^*$  space, where  $\Delta^* = \Delta D_c$  is the nondimensional sill height. The flow is separated to the right of each line. The dashed line indicates where the interface separates from the left-hand wall, where the depth is now equal to zero. The diagrams are valid for any type of flow, controlled or noncontrolled, and may be used as follows: Enter the upstream value of the channel width where the bottom is flat ( $\Delta^*=0$ ). Draw a line in the  $t-\Delta^*$  space corresponding to the geometric changes of the channel when moving up the sill. If this line crosses the solid curve for the particular value of  $\hat{D}_c$  (which is given), the flow separates at this point. It will remain separated as long as the "topography" line lies to the right of the solid curve. The flow reattaches if the solid line is crossed once again and the topography line lies to the left of it.

Two general results can be established from the theoretical considerations. First, no flow can separate from the right hand wall if the channel floor is flat ( $\Delta^*=0$ ), i.e., if only the width varies

(see Figure 2). Second, all controlled flows will reattach before reaching the sill crest. The latter statement evolves from equations (2) and (3) which show that the velocity at  $x=w/2$  cannot be less than zero at the control section. The only case for which the velocity at the right-hand wall equals zero at the control section is

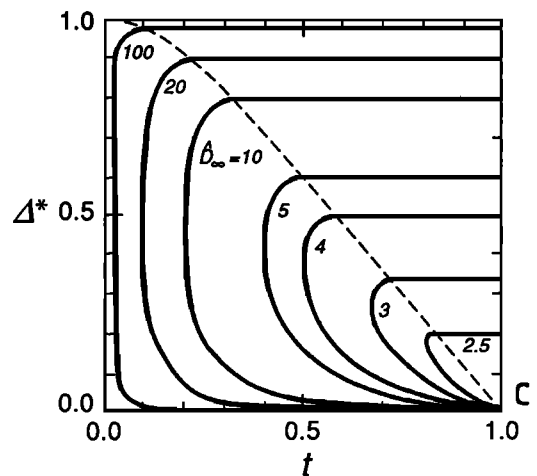
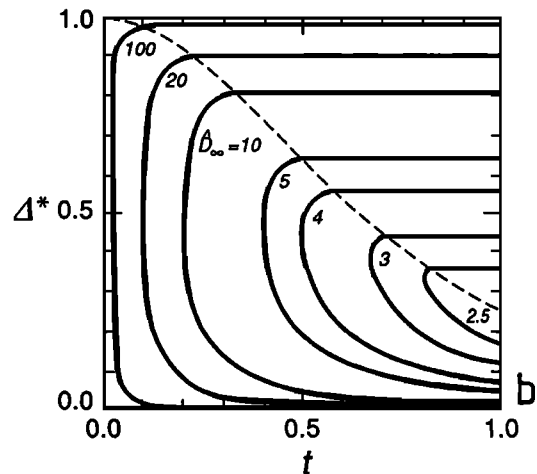
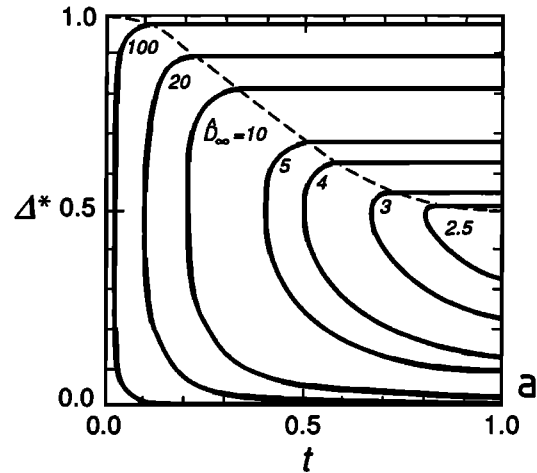


Figure 2. Curves for different values of  $\hat{D}_c$  dividing the separated flow from the nonseparated flow, for (a)  $\psi_1^* = -1/2$ , (b)  $\psi_1^* = 0$ , and (c)  $\psi_1^* = 1/2$ . The flow is separated to the right of each curve. The dashed line indicates where the depth at the left hand wall equals zero.

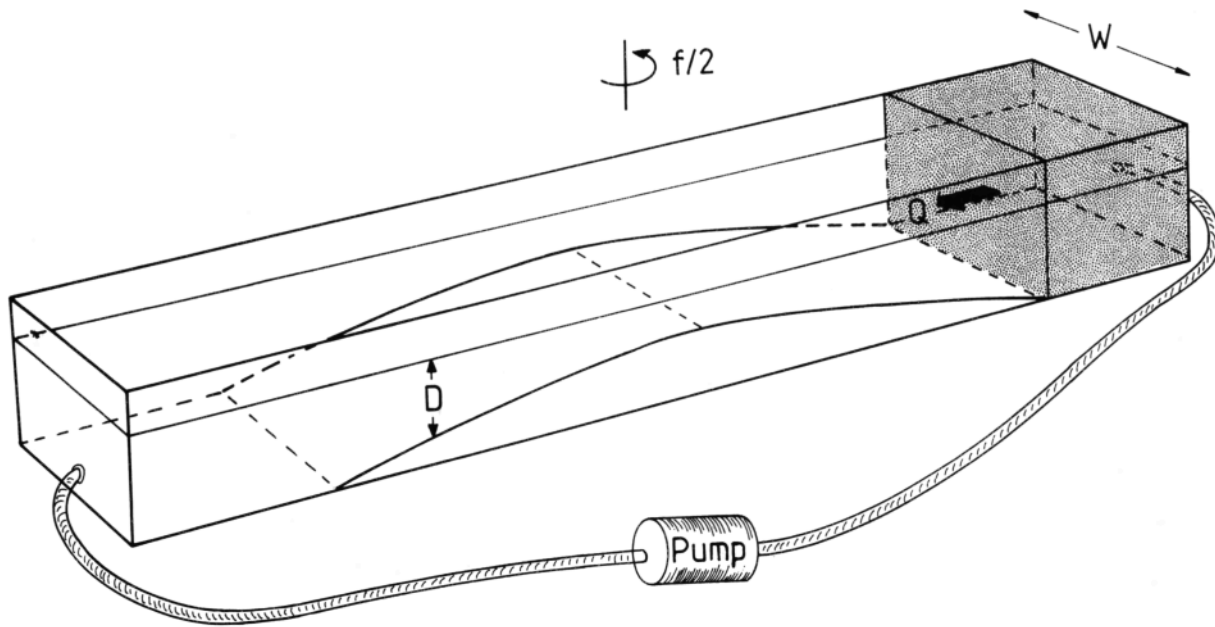


Figure 3. Geometry of the channel used in the experiment.

for  $D = (Qf/2g')^{1/2}$ , corresponding to  $D(-w/2)=0$ , that is when the lower layer ceases to wet the left-hand wall [cf. Gill, 1977].

When the flow separates from the right-hand wall, it is not evident what the potential vorticity should be in the area enclosed by the separating streamline. If the value of the potential vorticity is taken to be the same everywhere in the fluid [see, e.g., Gill, 1977; Borenäs and Pratt, 1994], the separated area is one of recirculation. Another possibility is to assume that the flow is stagnant within the separating streamline on which the velocity now must be zero [Borenäs, 1983]. For this case, the Bernoulli equation should be applied along the separating streamline and not along the real wall. Compared to the recirculation case, the downstream flow is now distributed over a greater width, and the velocities are consequently lower.

#### 4. Experimental Setup

The theoretical considerations described above will predict the separation features given the constancy of Bernoulli potential along streamlines, but this cannot be assured for closed streamlines. Thus laboratory experiments were conducted to determine what the flow configurations would be in a physically realized situation.

The experimental design was similar to that used by Whitehead [1986]. A tank, 1 m long and 0.15 m wide, was used (see Figure 3), and a sill of parabolic shape was placed at the center of it. The total length of the sill was 0.5 m, and the maximum height was 0.06 m. The tank was filled with a layer of water which measured 0.08 m on the upstream side of the sill. It was desirable to have a flow that was controlled by the sill, since for such a flow, downstream disturbances cannot propagate to the upstream side of the sill and influence the upstream conditions. In principle a one-layer setup is possible, but to get controlled conditions at reasonable flow rates, a 0.03-m-thick layer of kerosene was poured on top of the water. The gravity was in this way reduced to  $g'=1.91 \text{ m s}^{-2}$ .

Water in the lower layer was pumped from the downstream side of the sill to an upstream reservoir, where it flowed through a

porous diffuser before entering the channel. The tank was mounted on a turntable, 1 m in diameter, which could rotate at various speeds. The flow rate and rotation period were chosen so as to make the flow critical. (Note that these two quantities are coupled and cannot be chosen independently.) Enough time was given for the fluid to spin up to the required rotation before any observations were made. The flow was visualized by adding thymol blue (which is amber when neutral) to the lower layer. Then NaOH was added to the fluid close to the outlet, creating a large pulse of dark blue fluid which could be followed. A camera was mounted over the tank, and pictures were taken over the sill area.

In designing the experiment, the geometry and parameters have to be chosen in such a way that the assumed value of the potential depth (which is taken to be identical to the upstream interior depth) is compatible with the assumptions made for a flow of constant potential vorticity [see Borenäs and Pratt, 1994]. Consequently, the kinetic energy, predicted by hydraulic theory, must be small compared to the potential energy in the upstream basin where  $\Delta^*=0$ . Likewise, must the velocity shear in the reservoir be small compared to the rotation. Keeping these restrictions in mind, the main part of the experiment was carried out for four different values of the nondimensional channel width,  $w^*=w/R$ . These values were 0.25, 0.30, 0.35 and 0.39. The maximum relative sill height  $\Delta^*=\Delta/D_\infty$  was kept constant at 0.75. The experimental data are given in Table 1.

In the first set of experiments it was established from the

Table 1. Values of the Parameters Used in the Main Part of the Experiment

$w^*$	$f, \text{ s}^{-1}$	$Q, \times 10^{-4} \text{ m}^3 \text{ s}^{-1}$
0.25	1.30	2.49
0.30	1.56	2.28
0.35	1.82	2.06
0.39	2.03	1.87

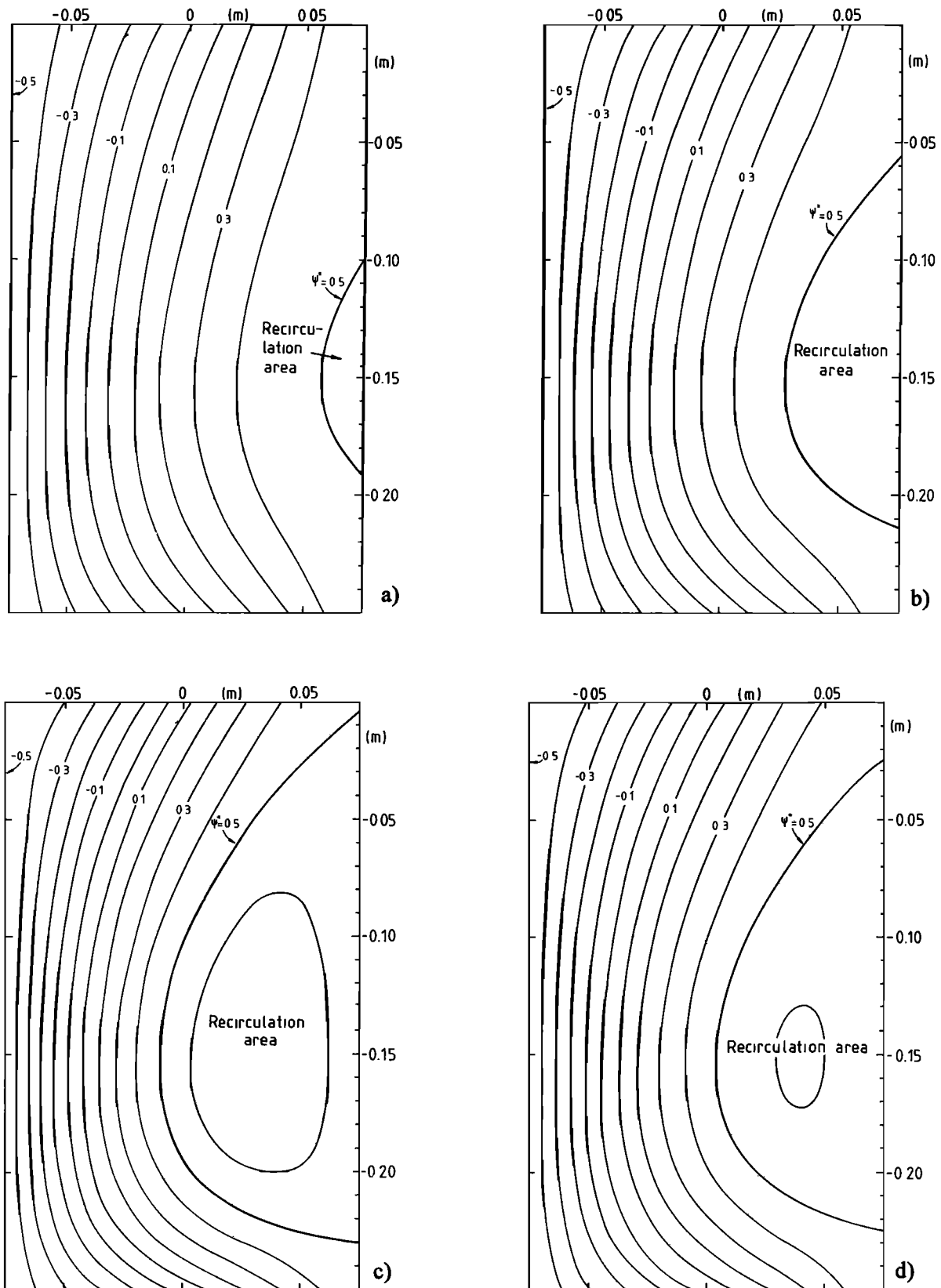


**Figure 4.** Lines of constant  $\psi^*$  for the case  $\psi^*_i=1/2$ , with potential vorticity constant throughout the fluid; for, (a)  $w^*=0.25$ , (b)  $w^*=0.30$ , (c)  $w^*=0.35$ , and (d)  $w^*=0.39$ .

The flow enters at the bottom of each panel ( $\Delta^*=0$ ) and the crest ( $\Delta^*_c=0.75$ ) is at the top.

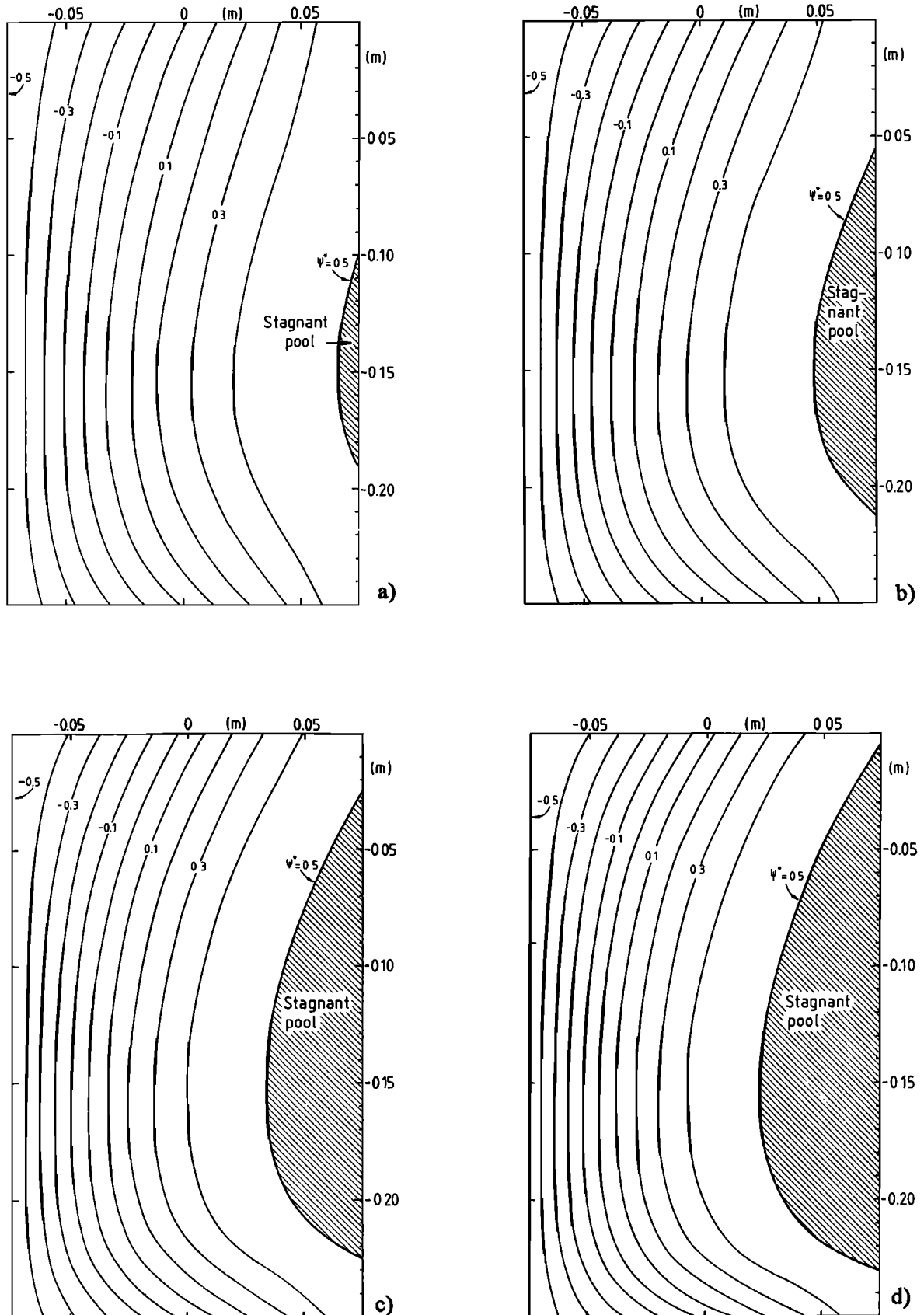


**Figure 5.** Lines of constant  $\psi^*$  for the case  $\psi^*_i = 1/2$ , with the separating streamline encompassing a stagnant pool of fluid, for, (a)  $w^* = 0.25$ , (b)  $w^* = 0.30$ , (c)  $w^* = 0.35$ , and (d)  $w^* = 0.39$ . The flow enters at the bottom of each panel ( $\Delta^* = 0$ ) and the crest ( $\Delta^*_c = 0.75$ ) is at the top.

photos where the separation and reattachment took place. The length and the width of the area was also measured. Some additional runs were made in order to determine the minimum value of  $w^*$  for which separation occurred. In the second part of the experiment the flow field in the separation area was studied.

## 5. Theoretical and Observed Flow Field

The theoretical flow field chosen for comparisons with the experimental results was one with  $\psi_1^* = \psi/Q = 1/2$ . This is the type of flow that would result from a dam break situation [see Gill, 1977]. The choice is not crucial, since for the widths here considered the velocity profile upstream the sill is quite insensitive to the value of  $\psi_1^*$ . This fact is also demonstrated in Figure 2; for small values of the parameter  $t$  there is little difference between the three graphs.

As was mentioned in section 3, the theoretical flow field also depends on the assumptions made about the separated area. This is illustrated in Figures 4 and 5, where Figure 4 pertains to the case of a recirculation area to the right of the separating streamline (the potential vorticity is constant throughout the fluid), and Figure 5 shows the flow field when  $\psi^* = \psi/Q = 1/2$  encloses a stagnant pool. The separated area, which is given by the thick solid line, is apparently much wider when a recirculation is present. It should be noted, though, that for a given value of  $w^*$ , the points of separation and reattachment are the same for the two different configurations. Figures 4 and 5 also show that both the width and the length of the separated area increase for larger values of  $w^*$ , hence intensifying the downstream part of the flow.

The pictures taken during the experiment showed several features similar to the theoretical predictions. First, no stagnation point was found when the nondimensional width  $w^*$  of the channel was below a certain value. Second, the separation area was larger for larger values of  $w^*$ . It was also clearly demonstrated that the shape of the separation area was asymmetric, in accordance with the theory. As an example, the experimental flow field for  $w^* = 0.35$  is shown in Plate 1, which could be compared with the theoretical flow field presented in Figures 4 and 5.

In order to facilitate the interpretation of the photos, hypothetical particle paths were calculated from theory for the

various nondimensional channel widths, assuming that the separation area was one of recirculation. Judging from the observed width of the region enclosed by the streamline  $\psi^* = 1/2$ , this scenario seemed to give a better description of the flow field than the one of a stagnant pool (compare Figure 4 and Plate 1). In this way it was possible to determine the time the fluid theoretically required to reach the point of separation, follow the separation contour, and then reattach. The hypothetical particles were "released" at the edge of the parabolic bottom ( $y = -0.25$  m), at various cross channel positions. It turned out that a streamline emanating from  $x_0 = 0.0749$  m followed the separation area (given by  $\psi^* = 1/2$ ) quite closely, but for a streamline starting from a point only 1 mm further out from the wall, the distance to the points of stagnation was quite large.

A general result for particles released at  $x_0 = 0.0749$  m was that it took 3–4 revolutions to reach the sill crest. This is apparently the minimum time that has to elapse in the experimental setup (after the colored fluid has reached the edge of the sill) before any measurements should take place. However, since these particles are so close to the wall, frictional effects have to be important with a further slowing down. Therefore measurements were made both after four and eight rotations.

In Figure 6 the length between the stagnation point and the reattachment point on the right-hand wall is shown as a function of the nondimensional width  $w^*$ . The solid line shows the theoretical prediction, and for this particular setup, the flow remains attached to the right-hand wall as long as  $w^*$  is less than about 0.22. If  $w^*$  is increased above this value, the flow will separate from the wall for a certain length after which it reattaches. The length of the separated area (measured at the wall) increases with increasing  $w^*$ . The open and solid circles pertain to the experimental results obtained four and eight rotations respectively after the colored fluid has reached the edge of the sill. From the numerous photos taken during the experiment it was concluded that after a few rotations the fluid had reached the point of separation and that the position of this point was more or less constant thereafter. The position of the reattachment point continued to move upstream until eight rotations had elapsed; then its position changed very little as well. The figure demonstrates that the minimum value of  $w^*$  for which separation occurs was slightly smaller in the experiment but that the agreement between the theoretical curve and the experimental results was quite good.

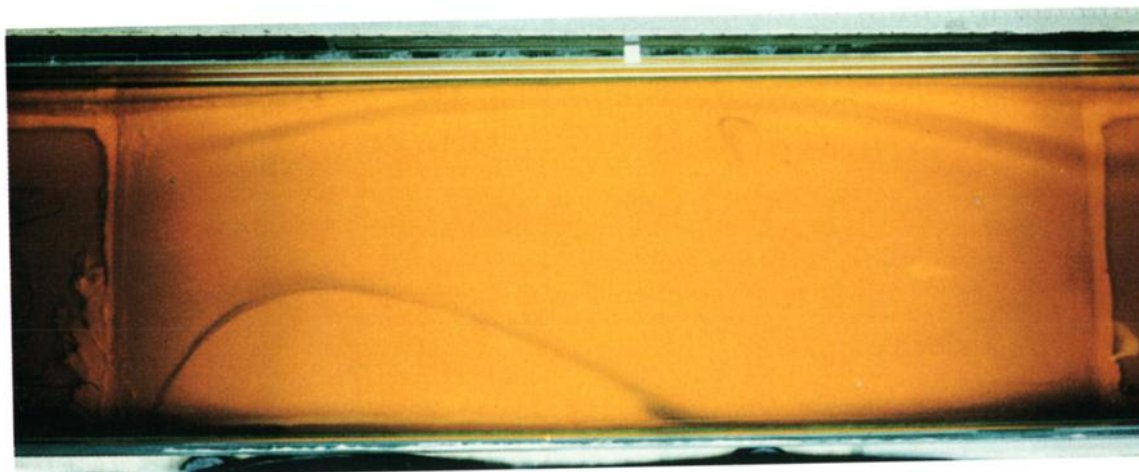


**Plate 1.** Experimentally observed separation area for  $w^* = 0.35$ . The flow is from left to right, and the photo (taken from above) covers the entire sill.

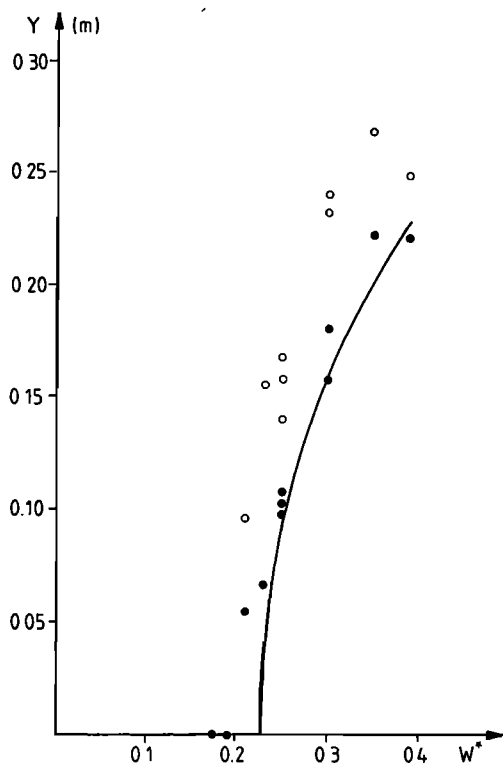


**Figure 6.** Length ( $Y$ ) of the separation area versus the nondimensional width. The theoretical curve is given by the solid line. Open and solid circles show the experimental results obtained four and eight rotations respectively, after the colored fluid has reached the edge of the sill.

## 6. The Flow in the Separation Area

In order to study the flow within the separated region more closely, a frame was mounted across the channel, with thin rods sticking down to a couple of millimeters above the bottom (above the Ekman layer). The position of the frame was chosen to be at  $y=0.15$  m, which would be across the center of the eddy predicted by the recirculation model. The visualization of the flow field was made by electrically produced dye using the pH model technique [see, e.g., Tritton, 1977].

It was again concluded that the stagnant pool model did not agree with the observed flow field, and that the fluid motions did not look like those predicted by the recirculation model. The velocities were typically much smaller in the experiment. For  $w^*=0.39$ , for example, the photos (taken at a rate of one picture per rotation) suggested that the velocities were about an order of magnitude less than the velocities calculated from the recirculation model. Furthermore, the flow pattern differed markedly from the simple eddy structure. The most characteristic feature was the presence of a cyclonic eddy which always covered the upstream half of the separated region. This feature is demonstrated in Plates 2a, 2b and 2c. (compare with Figure 4, which shows an anticyclonic eddy extending over the whole area.) The series of photos taken of the eddy shown in Plate 2b, indicated that the relative vorticity of this eddy was much less than  $f$  and that the potential vorticity did not correspond to the upstream value. Plates 2b and 2c also show a growing instability at the edge of the

separated region, usually starting at half the distance between the maximum separation width and the point of reattachment. The instability developed into a cyclonic eddy which was eroded at the edge by the cross-channel motions mentioned above. The velocities in this eddy were of the size as those in the upstream cyclonic eddy.

In some cases a reversed flow was found along the right-hand wall, starting close to the point of reattachment. An example of this pattern is given in Plate 2d. When meeting the cyclonic eddy, the flow left the wall and turned into an anticyclonic eddy, as shown in Plates 2e and 2f. The vortex pairs were found only for lower values of  $w^*$ , in which case the tendency for instabilities at the edge of the separation area seemed to be somewhat smaller. There were indications of reversed flows also for larger values of  $w^*$ , but for these widths the eddy generated by the instability dominated.

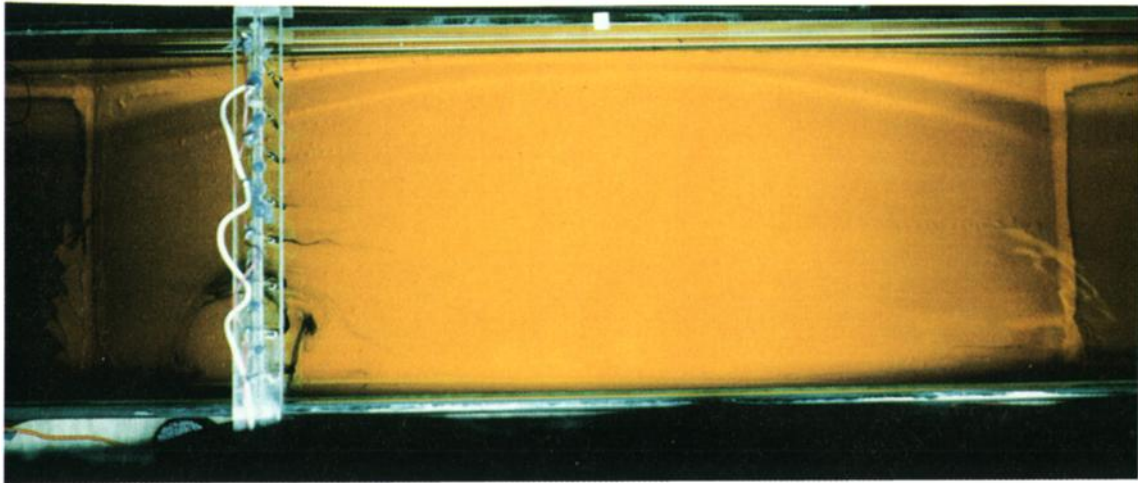
It should be pointed out that no color was injected in the separation area in the examples shown in Plates 2b, 2c, 2e and 2f. That is, the blue colored fluid we see within this area consists of upstream water.

## 7. Discussion

A theoretical study of upstream separation in a rotating channel flow has been undertaken. In addition, a series of experiments have been carried out in order to investigate whether separation actually takes place and if the theoretical assumptions usually made about the flow in areas of upstream separation are relevant or not. It has been demonstrated that the hypothesis that the flow is stagnant in the separated area, which would correspond to the least energetic state [Borenäs, 1983], does not agree with the experimental results. The flow circulated in the region, although quite slowly, and the width of the separated area was larger than predicted by the stagnant pool theory. The second hypothesis, that the separating streamline encloses a region of anticyclonic circulation, has also proven to be incorrect. Even though the shape and size of the separated region found in the experiments corresponded with the theoretical predictions, the circulation pattern differed quite markedly.

The motions found in the separated area are rather complicated. The vortex pairs may indicate that the total amount of relative vorticity is zero, as it would be in the absence of an outflow. However, the instability at the edge of the separated area prevents any conclusions about the generality of this pattern. It is beyond the scope of the present paper to provide detailed measurements of the flow in this region, but it is clear that the potential vorticity in the separated area differs from the upstream value and that steady rotating hydraulic theory cannot describe the fluid motions here. This conclusion is not totally surprising, considering that the basic assumptions in the theory are made for streamlines emanating from the upstream basin. What the value of the potential vorticity should be along the streamlines in an enclosed area is indeed an open question. Furthermore, it is quite likely that lateral friction is important in this region.

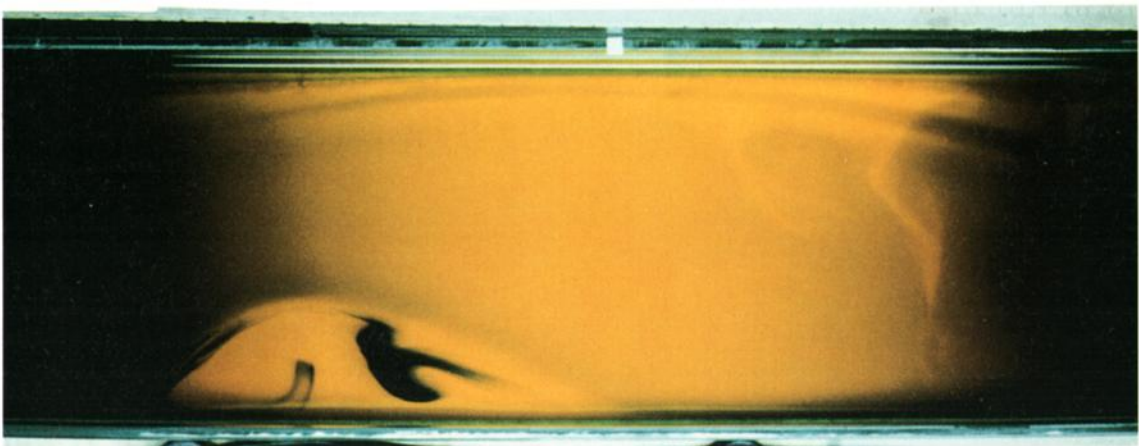
Any type of motion in an enclosed area would decay as a result of friction, eventually resulting in a pool of stagnant fluid, unless energy was drained from the main flow. Some of the potential energy the flow possesses at the entrance of the sill would then be lost to the eddies, which in turn would decrease the kinetic energy of the main flow. In order to get critical conditions at the sill, the upstream level would then have to readjust to a larger value. This means that for a given upstream depth the theoretically predicted



(a)

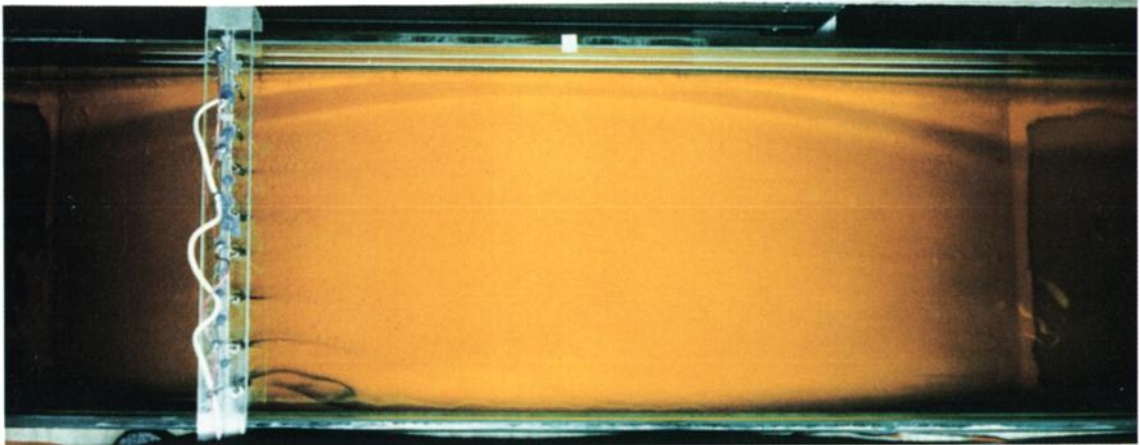


(b)

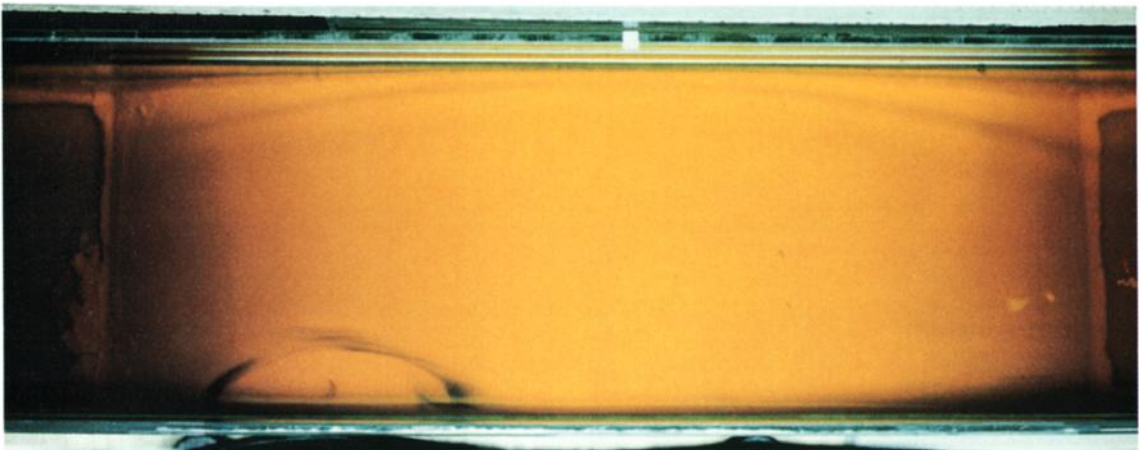


(c)

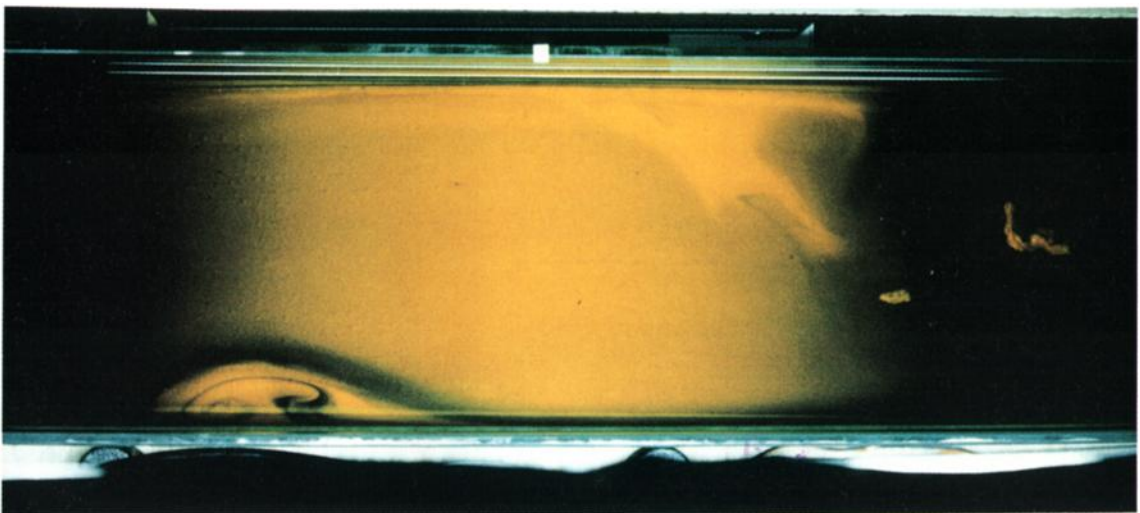
**Plate 2.** Examples of the experimentally observed streak lines in the area of separation, for, (a), (b)  $w^*=0.39$ , (c)  $w^*=0.30$ , (d), (e)  $w^*=0.25$ , and (f)  $w^*=0.23$ . The flow is from left to right and the photos, which are taken from above, cover the entire sill.



(d)



(e)



(f)

size of the controlled transport over the sill would be too large. It would therefore be advisable, when using rotating hydraulic theory for estimates of maximum transport, to check whether there is a possibility of upstream separation of the flow. Although the theory presented here pertains to a channel of rectangular cross section, the flow in a channel of parabolic cross section, for example, would exhibit the same type of flow pattern with areas of separation. Since it is required that variations in the downstream direction be gradual, the theory is not applicable for broad sill crests.

It is interesting to compare the theoretical and experimental results here obtained with the flow pattern presented by *van Aken* [1988] in the deep water of the Faroese Channels (see Figure 7). An inverse method was used in that paper and the calculations resulted in a large area of anticyclonic motions in the eastern part of the Faroe Bank Channel and a cyclonic circulation in the southern part of the Faroe-Shetland Channel. Both circulation cells are found in the right-hand part of the respective channel. In

an attempt to apply the theory of separation to this area, the value of  $\hat{D}_\infty$  can be determined assuming that the flow is controlled by the sill in the Faroe Bank Channel. If the reservoir depth  $D_\infty$  of the lower layer is taken to be 1300 m and the sill height above the reservoir depth is 900 m, then the nondimensional height  $\Delta^*$  of the sill is  $\sim 0.7$ . If, furthermore, the width of the channel at the sill is about 15 km, corresponding to  $t \sim 0.4$ , then the value of  $\hat{D}_\infty$  for a controlled flow is  $\sim 6.7$  [cf. *Gill*, 1977]. (Here  $g' = 4.3 \times 10^{-3} \text{ m s}^{-2}$  and  $f = 1.27 \times 10^{-4} \text{ s}^{-1}$  [cf. *Borenäs and Lundberg*, 1988]). The width of the channel decreases from  $\sim 70$  km in the Faroe-Shetland Channel to  $\sim 15$  km at the sill, corresponding to a  $t$  decreasing approximately from 0.95 to 0.4. Figure 2 demonstrates that according to the theory, the flow will separate for a low value of the relative sill height and remain separated until it approaches the top of the sill. The calculated flow pattern by *van Aken* [1988], with the various recirculation cells along the channels, gives some support to the results presented here.

Another point could be made here concerning the flow rate. The value of  $\hat{D}_\infty$ , around 6.7, corresponds to a controlled flow rate of  $\sim 2.5$  Sv (with the values of  $g'$  and  $f$  given above). The observed flow rate is reported to be about 1.5-2 Sv [*Saunders*, 1990; *Borenäs and Lundberg*, 1988], which is less than the calculated value. One explanation could be that, as discussed earlier in this section, the available potential energy, represented by the upstream height of the lower layer, is to some extent used to maintain the eddies on the right-hand flank, thereby decreasing the predicted flow rate. Further investigations would be needed to get an estimate of how much of the energy the eddies use.

**Acknowledgments.** We thank Robert Frazel for help with the laboratory apparatus and the photography, and Agneta Malm for technical assistance. The comments from the reviewers are also appreciated. Partial support for the laboratory study was by the Coastal, Arctic and Physical Oceanography sections of the Office of Naval Research under contract N00014-89-J-1037. The work was also supported by the Swedish Natural Science Research Council under contracts G-GU-9811-305 and G-GU-09811-307. A travel grant from the Wallenberg Foundation is also acknowledged.

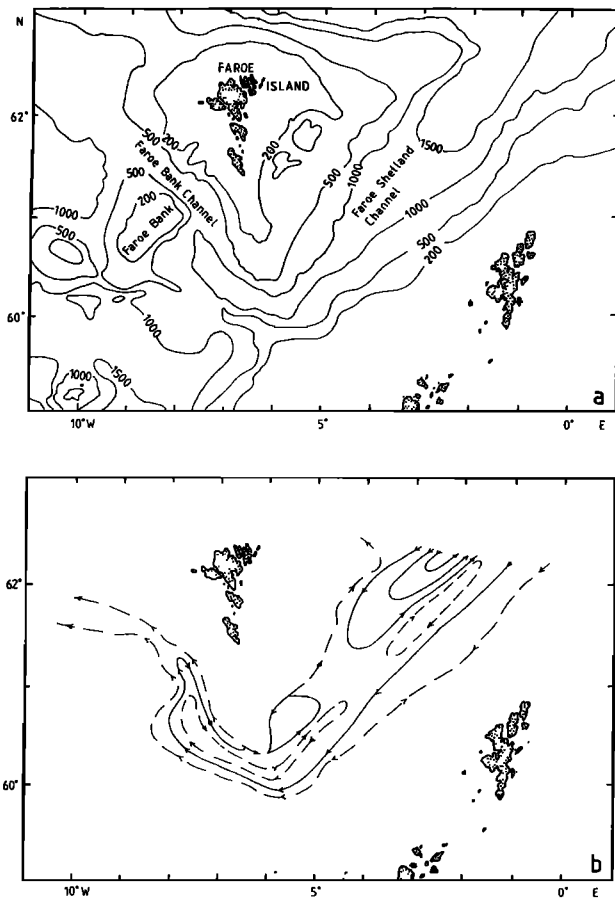


**Figure 7.** (a) Map showing the bathymetry in the area of the Faroese Channels. (b) Streamlines, obtained by *van Aken* [1988], showing the flow field in the bottom layer. The transport between the solid lines is  $1 \times 10^9 \text{ kg s}^{-1}$ , and the dashed lines show the position of the stream function values halfway between the solid lines. The dash-dotted lines indicate the position where the layer is bounded by the topography. Reprinted from *Deep Sea Res.*, 35, H. M. van Aken, Transports of water masses through the Faroese Channels determined by an inverse method, 595-617, 1988, with kind permission from Elsevier Science Ltd, The Boulevard, Langford Lane, Kidlington OX5 1GB, UK.

## References

- Borenäs, K., Subcritical rotating channel flow across a ridge, in *Coastal Oceanography*, edited by H.G. Gade, A. Edwards, and H. Svendsen, pp. 363-372, Plenum, New York, 1983.
- Borenäs, K. M., and P. A. Lundberg, On the deep-water flow through the Faroe Bank Channel, *J. Geophys. Res.*, 93, 1281-1292, 1988.
- Borenäs, K. M., and L. J. Pratt, On the use of rotating hydraulic models, *J. Phys. Oceanogr.*, 24, 108-123, 1994.
- Garrett, C. J. R., and B. Toulany, Sea level variability due to meteorological forcing in the northeast Gulf of St. Lawrence, *J. Geophys. Res.*, 87, 1968-1978, 1982.
- Gill, A. E., The hydraulics of rotating-channel flow, *J. Fluid Mech.*, 80, 641-671, 1977.
- Pratt, L. J., Rotating shocks in separated laboratory channel flow, *J. Phys. Oceanogr.*, 17, 483-491, 1987.
- Pratt, L. J., and P. A. Lundberg, Hydraulics of rotating strait and sill flow, *Annu. Rev. Fluid Mech.*, 23, 81-106, 1991.
- Saunders, P. M., Cold outflow from the Faroe Bank Channel, *J. Phys. Oceanogr.*, 20, 29-43, 1990.
- Schlichtholz, P., and A. Jankowski, Hydrological regime and water volume transport in the Faroe-Shetland Channel in summer of 1988 and 1989, *Oceanol. Acta*, 16, 11-22, 1993.
- Shen, C. Y., The rotating hydraulics of open-channel flow between two basins, *J. Fluid Mech.*, 112, 161-188, 1981.

- Tritton, D. J., *Physical Fluid Dynamics*, Van Nostrand Reinhold, New York, 1977.
- van Aken, H. M., Transports of water masses through the Faroese Channels determined by an inverse method, *Deep Sea Res.*, 35, 595-617, 1988.
- Whitehead, J. A., Jr., Rotating critical flows in the ocean, in *Proceedings of the Second International Symposium on Stratified Flows*, edited by McClimans., pp. 72-80, Tapir, Trondheim, Norway, 1980.
- Whitehead, J. A., Flow of homogeneous rotating fluid through straits, *Geophys. Astrophys. Fluid Dyn.*, 36, 187-205, 1986.
- Whitehead, J. A., A. Leetmaa, and R. A. Knox, Rotating hydraulics of strait and sill flows. *Geophys. Fluid Dyn.*, 6, 101-125, 1974.
- K. M. Borenäs, Department of Oceanography, Earth Sciences Centre, Göteborg University, S-41381 Göteborg, Sweden. (e-mail: kabo@oce.gu.se)
- J. A. Whitehead, Department of Physical Oceanography, Woods Hole Oceanographic Institution, Woods Hole, MA 02543.

(Received October 30, 1995; revised August 18, 1997; accepted September 9, 1997.)